

## The Energetics of Asian Summer Monsoon

P. L. S. RAO<sup>1</sup>

*Abstract*—In this paper, we examine the large-scale balances of kinetic energy, vorticity, angular momentum, heat and moisture over the Asian summer monsoon region. The five year (1986–1990) uninitialized daily analyses for the summer season comprising June, July and August (JJA), produced at the European Centre for Medium Range Weather Forecasts (ECMWF) under the aegis of Tropical Ocean and Global Atmosphere (TOGA) have been considered to carry out the study.

The following features characterize the Asian summer monsoon domain. It acts as the source of kinetic energy as well as vorticity, and sink of heat and moisture. Kinetic energy and vorticity are produced in the monsoon region and transported horizontally. On the contrary, heat and moisture are transported into the monsoon region. The zonal and meridional components of adiabatic generation of kinetic energy contribute to the production of kinetic energy over the Arabian Sea and Bay of Bengal, respectively. The horizontal advection of relative vorticity is balanced by sub-grid scale generation. The angular momentum generated due to pressure torque (east-west pressure gradient) is balanced by the flux convergence of omega momentum. Further, the angular momentum budget delineates that flux convergence of relative momentum is necessary to maintain the surface westerlies against the friction. The horizontal convergence of heat and moisture facilitates enhancement of diabatic heating, and also leads to the formation of diabatic heat sources, which are crucial to sustain the summer monsoon circulation.

**Key words:** Monsoon, kinetic energy, heat, moisture, vorticity and angular momentum.

### 1. Introduction

The Asian summer monsoon represents a longitudinal asymmetric component of the general circulation of the atmosphere, characterized by periodic reversal of wind regimes, movements of jet streams and semi-permanent high and low pressure areas. A well-known basic drive for the monsoon circulation is provided by intense and persistent differential heating between the land and ocean. The summer monsoon circulation over the Indian subcontinent and adjoining seas is characterized by convergence of mass and moisture in the lower levels and strong divergence aloft. The monsoon circulation is triggered by a sequence of events. The formation of a heat low over northwest India precedes transport of moisture into the land mass (RAO *et al.*, 1981). This is followed by convergence of heat

---

<sup>1</sup> IBM India Research Laboratory, Indian Institute of Technology, Hauz Khas, New Delhi-110016, India. E-mail: rpolasam@in.ibm.com

(MOHANTY *et al.*, 1983). Consequently, both give rise to profound cumulus convection, which in turn enhances diabatic heating. This enables abundant generation of available potential energy (APE). The establishment of monsoon circulation is noted by a sudden and persistent rise in adiabatic conversion of APE to kinetic energy (MOHANTY *et al.*, 1999) and also evinced by a steep rise in kinetic energy (KRISHNAMURTI *et al.*, 1981; PEARCE and MOHANTY, 1984). Albeit, the onset of the summer monsoon takes place towards the end of May, and the circulation prevails through the end of September.

The prominence of the diagnostic studies employing observed data sets is well recognized as an important GARP problem (PEARCE, 1979; KUNG and SMITH, 1974). The advent of several field experiments over the Asian summer monsoon region necessitated a comprehensive understanding of dynamics and energetics of the Asian summer monsoon to ameliorate its simulation/prediction. Although a large number of studies are reported on diagnostic aspects of the atmosphere, very few are related to the Asian summer monsoon. The First GARP Global Experiment (FGGE) provided an opportunity to undertake detailed studies over the Asian summer monsoon region (MOHANTY *et al.*, 1982a,b, 1983; PEARCE and MOHANTY, 1984; GEORGE and MISHRA, 1993). Currently, the availability of globally analyzed upper air meteorological fields from various operational weather forecasting centers around the world, enriches the scope of understanding the mechanisms of the otherwise data sparse tropics, especially the monsoon region. Despite the fact that some aspects of energetics and dynamics were addressed in earlier studies (MOHANTY and RAMESH, 1994; Ramesh *et al.*, 1996), a comprehensive understanding is necessary to interpret the Asian summer monsoon circulation in the extended range/seasonal scale simulations. Further, it is also crucial to diagnose the source of errors associated with the seasonal scale simulations and offer plausible explanations. In this vein, we examined kinetic energy, vorticity, angular momentum, heat and moisture budgets over the Asian summer monsoon domain.

## 2. Methodology

The budget equations are obtained from the equations of motion and other conservation laws, which the atmosphere obeys and represented in the flux form with pressure as the vertical coordinate. It is well known that any time mean atmospheric circulation consists of a stable component, which remains almost constant or varies slowly over a time period, which is called the mean part, and another rapidly varying component, which changes rapidly over a time period, which is called the eddy part. In general, tropical circulations are dominated by the mean component of the flow and extratropical circulations are dominated by the eddy component of the flow. Since the Asian summer monsoon circulation is predominantly driven by the mean component of the flow, we have bifurcated the

time mean budgets into the respective mean and eddy budgets. In this study, we have elucidated only the mean budgets. The various budget equations are expressed in the flux form with pressure as the vertical coordinate. The kinetic energy equation is expressed as

$$\frac{\partial \overline{K_M}}{\partial t} + \nabla \cdot (H_0 + H_1) + \frac{\partial}{\partial P} (\overline{K_M + \bar{V}V'})\omega = -\bar{V} \cdot \nabla \bar{\phi} - C(K_M, K_T) + \bar{V} \cdot \bar{F} \quad (1)$$

where  $K_M = \frac{1}{2} \bar{V}^2$  kinetic energy of the mean flow,  $K_T = \frac{1}{2} V'^2$  kinetic energy of the eddy flow.

Various notations used in the equation are given below.

$$\begin{aligned} H_0 &= K_M \bar{V} \\ H_1 &= \overline{(\bar{V} \cdot V')V'} \\ C(K_M, K_T) &= C_H(K_M, K_T) + C_v(K_M, K_T) \\ C_H(K_M, K_T) &= -\frac{\overline{u'u'}}{a \cos \varphi} \frac{\partial \bar{u}}{\partial \lambda} - \frac{\overline{u'v'} \cos \varphi}{a} \frac{\partial}{\partial \varphi} \left( \frac{\bar{u}}{a \cos \varphi} \right) \\ &\quad - \frac{\overline{u'v'}}{a \cos \varphi} \frac{\partial \bar{v}}{\partial \lambda} - \frac{\overline{v'v'}}{a} \frac{\partial \bar{v}}{\partial \varphi} + \frac{\overline{u'u'}}{a} \frac{\bar{v} \tan \varphi}{a} \end{aligned}$$

and

$$C_v(K_M, K_T) = -\overline{u'\omega'} \frac{\partial \bar{u}}{\partial P} - \overline{v'\omega'} \frac{\partial \bar{v}}{\partial P} .$$

The first term on the left of equation (1) designates the local rate of change of the kinetic energy. The second and third terms describe the horizontal and vertical divergence fluxes of kinetic energy, respectively. Similarly, the first term on the right denotes the conversion of available potential energy to kinetic energy through the action of pressure forces (adiabatic generation of kinetic energy). The second term evinces the exchange of  $K_M$  to  $K_T$  and vice versa which arises basically from the large-scale horizontal and vertical Reynold's stresses. The last term signifies the dissipation of kinetic energy by the turbulent frictional processes.

The vorticity budget equation is designated as

$$\frac{\partial \bar{\zeta}}{\partial t} + \nabla \cdot (\bar{\zeta} \bar{V}) + \beta \bar{v} + \frac{\partial (\bar{\zeta} \bar{\omega})}{\partial P} = -(\bar{\zeta} \bar{D}) - k \cdot \left( \nabla \omega \times \frac{\partial v}{\partial P} \right) + \bar{Z} . \quad (2)$$

The first term on the left of equation (2) represents the local rate of change of relative vorticity. The second and third terms indicate the horizontal fluxes of relative and planetary vorticity, respectively. The fourth term describes the vertical flux of relative vorticity. Similarly, the first and second terms on the right-hand side evince the vorticity generation due to stretching and tilting, respectively. The final term

designates the residue of vorticity (i.e., generation/dissipation from sub-grid scale processes).

The angular momentum budget equation is illustrated as

$$\frac{\partial \bar{M}}{\partial t} + \nabla \cdot (\bar{M} \bar{V}) + \frac{\partial (\bar{M} \bar{\omega})}{\partial P} - f \bar{v} a \cos \varphi = - \frac{\partial \bar{\phi}}{\partial \lambda} + \delta \bar{\phi} + \bar{F}_\lambda, \quad (3)$$

where  $\bar{M} = \bar{u} a \cos \varphi$ .

In the equation (3), the first term on the left designates the local rate of change of relative momentum. The second, third and fourth terms describe the horizontal flux of relative momentum, vertical flux of relative momentum and horizontal flux of  $\Omega$  momentum, respectively. In the same manner, the first term on the right designates the pressure torque (i.e., east-west pressure gradient), the second term indicates the generation/destruction of momentum due to mountain torque. And the last term describes the frictional destruction of momentum.

The sensible heat energy budget equation is written as

$$\frac{\partial (\bar{C}_p \bar{T})}{\partial t} + \nabla \cdot (C_p \bar{T} \bar{V}) + \frac{\partial (C_p \bar{\omega} \bar{T})}{\partial P} - \bar{\omega} \bar{\alpha} = \bar{Q}_H. \quad (4)$$

In equation (4), the first term on the left describes the local rate of change of enthalpy. The second and third terms designate the horizontal and vertical fluxes of heat, respectively. The fourth term indicates the adiabatic conversion of available potential energy to kinetic energy. The term on the right describes the contributions from all diabatic processes in the atmosphere, namely radiation, condensation, evaporation of falling rain drops and turbulent transfer of sensible heat.

The latent heat energy budget equation is denoted as

$$\frac{\partial (\bar{L} \bar{q})}{\partial t} + \nabla \cdot L \bar{q} \bar{V} + \frac{\partial (L \bar{\omega} \bar{q})}{\partial P} = \bar{Q}_L. \quad (5)$$

In equation (5), the first term on the left describes the local rate of change of latent heat energy. The second and third terms represent the horizontal and vertical fluxes of latent heat energy, respectively. Similarly, the term on the right connotes the moisture source/sink, which comprises diabatic heating due to latent heat released from evaporation and condensation as well as the turbulent transfer of latent heat.

### 3. Data and Scheme of Analysis

The present study is carried out making use of an uninitialized daily analysis (1200 UTC) of ECMWF for five (1986–1990) summer seasons comprising June,

July and August. The data for the Asian summer monsoon region (45°N–15°S, 30°E–120°E) are extracted from the global analysis. The basic meteorological fields considered for the study include geopotential, wind, temperature and moisture at ten mandatory pressure levels (1000, 850, 700, 500, 400, 300, 250, 200, 150, 100 hPa). The special global analyzed data sets generated at the ECMWF under the international program on TOGA with a horizontal resolution of 2.5° on a regular latitude/longitude grid are made use of. The details of the ECMWF operational model are provided in the studies of JARRAUD and SIMMONS (1984), and SIMMONS *et al.* (1989). The uninitialized mass and velocity fields produced at ECMWF are of good quality and suitable for diagnostic studies. This fact was emphasized in various earlier studies (KANAMITSU, 1980; KUNG and TANAKA, 1983; JULIAN, 1984; Chen *et al.*, 1988).

The initialized vertical velocity field obtained from the nonlinear normal mode initialization and stored in the ECMWF archives does not represent true vertical motions in the tropics (KANAMITSU, 1980; MOHANTY *et al.*, 1989). Further, an intercomparison study (KUNG and TANAKA, 1983) indicates that the vertical motion of the ECMWF analyses is underestimated mainly over the rising branch of the Hadley circulation in comparison with that of the GFDL archives. It was also noted (JULIAN, 1984) that the horizontal wind fields generated by the ECMWF analyses represent a reasonable planetary scale divergent circulation over the tropics. Hence, instead of using the  $\omega$  field from the ECMWF data sets, the uninitialized wind fields have been used to derive the  $\omega$  field using the kinematic technique. In the kinematic method, the main problem is that of the accumulated biased errors involved in the computation of divergence from the wind components. A technique suggested by O'BRIEN (1970) has been used in the study to adjust the divergence in such a way that its vertically integrated value in any particular column of the atmosphere becomes zero. The vertical velocity ( $\omega$ ) values computed by the kinematic method described above have been used in the calculations of the various budgets.

In this study, the dynamic and thermodynamic budgets are computed using the daily analyzed fields of five summer monsoon seasons (JJA). Although we have analyzed mean as well as eddy components of all these budgets, the discussion invariably pertains to the mean component as the contribution of transient eddies to the time mean is one order less than the mean. The terms representing the local rate of change of various quantities have negligible contribution towards the respective budgets. The various space derivatives are evaluated by the centered difference scheme (second order) and the time derivatives are computed using the leap frog scheme. Further, trapezoidal rule has been used in the vertical integrations. The results at each regular latitude/longitude grid points are averaged both in zonal and meridional directions to construct vertical profiles, sectorial averages over the summer monsoon region and are also integrated vertically (1000–100 hPa) to derive net tropospheric geographical distributions.

### 4. Results and Discussion

The comprehensive analysis of energetics associated with the stable component of the Asian summer monsoon circulation is presented as follows.

#### 4.1. Mean Circulation Features

The mean wind at 850 and 150 hPa is depicted in Figure 1. The significant features observed in the wind field consist of low level jet (Somali Jet) and the upper level tropical easterly jet (TEJ). Both are in good agreement with climatology (NEWELL *et al.*, 1972; RAO, 1976). The distribution of mean wind field at 850 hPa depicts Southern Hemispheric trades with a speed of  $10\text{ ms}^{-1}$  ( $45^{\circ}\text{E}$ – $100^{\circ}\text{E}$ ), a strong cross-equatorial flow into the Northern Hemisphere off the Somali coast and a strong zone of westerlies over the Arabian Sea and Bay of Bengal ( $15\text{ ms}^{-1}$ ). Wind field distribution at 150 hPa is characterized by a strong and elongated anti-cyclone centered over Tibet ( $30^{\circ}\text{N}$ ) in the Northern Hemisphere. Two contrasting wind regimes present on either side of the Tibetan anti-cyclone, i.e. a westerly wind regime (sub-tropical westerly jet) towards the north (not shown in Fig. 1b) and an easterly

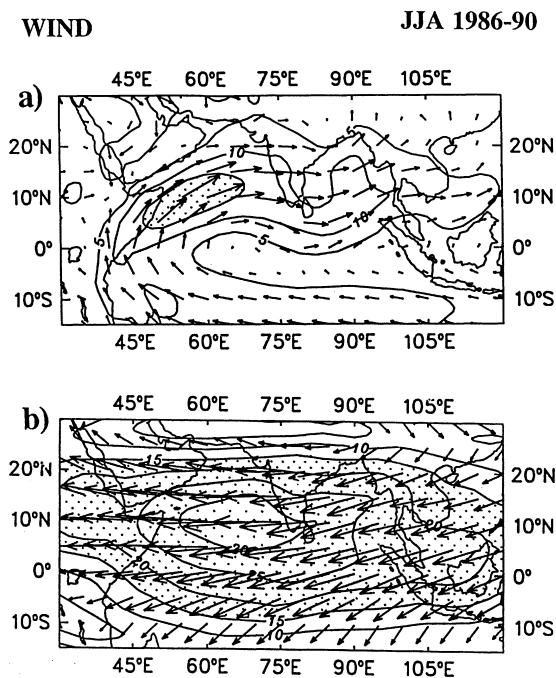


Figure 1

Wind field for JJA, 1986–1990. (a) 850 hPa, (b) 150 hPa, [contour interval;  $5\text{ ms}^{-1}$ , magnitudes larger than  $15\text{ ms}^{-1}$  are shaded].

regime (Tropical Easterly Jet) to the south, are the most prominent features of the Asian summer monsoon. The zone of easterlies extends over Indonesia, the Bay of Bengal, India, Arabian Sea, Africa and equatorial Indian Ocean, with a core of a maximum (about  $30 \text{ ms}^{-1}$ ) approximately  $5\text{--}15^\circ\text{N}$  over the southeast Arabian Sea and the adjoining Indian peninsula.

In order to delineate the characteristic circulation features of the Asian summer monsoon in the vertical plane, the sectorial ( $30^\circ\text{E}\text{--}120^\circ\text{E}$ ) pressure-latitude cross sections of zonal wind ( $u$ ), meridional wind ( $v$ ), omega ( $\omega$ ), and divergence ( $D$ ) are presented in Figure 2. The features depicted by zonal wind (Fig. 2a) include low-level westerlies pervading the entire monsoon region up to 500 hPa level with a jet located around 850 hPa level. Above that, a strong tropical easterly jet with a core of  $27 \text{ ms}^{-1}$  around 150 hPa level, followed by a westerly jet in the upper troposphere at 200 hPa level in the extra-tropics are also noticed. The subtropical jet is clearly discernable around  $40^\circ\text{N}$  in the extra-tropics. The characteristic strong low-level easterlies are noticed in the Southern Hemispheric tropics. The salient features pertaining to meridional wind (Fig. 2b) are cross-equatorial flow in the lower troposphere and return flow in the upper troposphere. Stronger return flow is indicated by the analysis compared to NEWELL'S (1972) climatology. The lower and upper level maxima are noticed around  $10^\circ\text{S}$ . The vertical velocity (Fig. 2c) reveals interesting features. The whole monsoon region is characterized by a rising motion

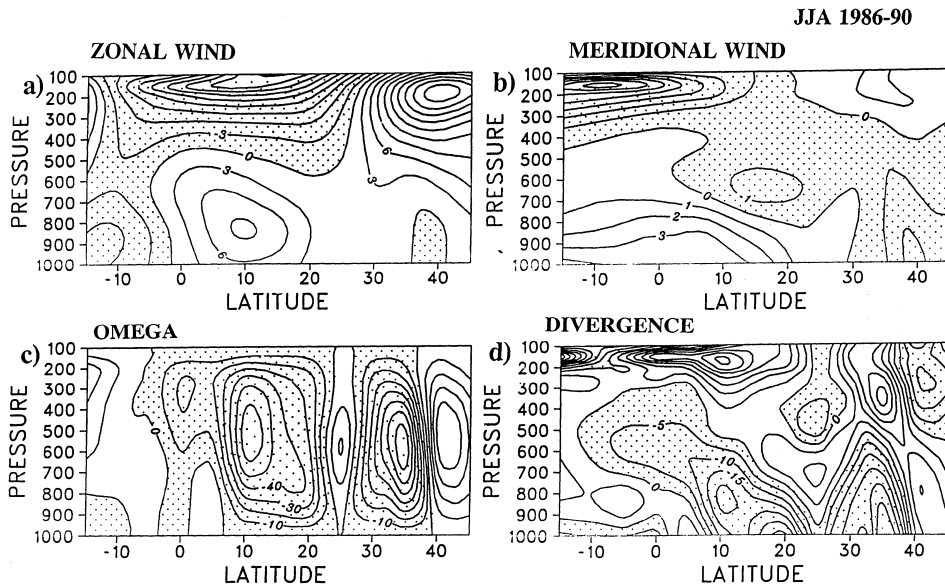


Figure 2

Sectorial ( $30^\circ\text{E}\text{--}120^\circ\text{E}$ ) mean pressure-latitude cross sections for JJA, 1986–1990. (a) Zonal wind,  $\text{ms}^{-1}$ , (b) meridional wind,  $\text{ms}^{-1}$ , (c) omega,  $10^{-3} \text{ Pa s}^{-1}$ , (d) divergence,  $10^{-6} \text{ s}^{-1}$  [contour interval for (a): 3; for (b): 1; for (c): 10; and for (d): 5; negative values are shaded].

with two maxima. The primary around 600 hPa level at 35°N, and the secondary around 500 hPa level at 10°N. The vertical velocity shows a small subsidence zone around 25°N. Another subsidence zone is noted between 5°S–15°S. However, the monsoon climatology shows a rising motion in this region. The divergence (Fig. 2d) depicts that the entire monsoon region is characterized by strong convergence in the lower troposphere and strong divergence in the upper troposphere. On the contrary, in the extra-tropics north of 40°N, the reverse is noticed. The low-level convergence exhibits two maxima around 20°N and 35°N, and the upper level divergence maximum is discerned around 10°N at 200 hPa level. A small divergence zone is detected in the lower levels around 25°N, which is in agreement with the subsidence observed in the vertical velocity.

#### *4.2. Kinetic Energy Budget*

The maintenance and intensity of the general circulation of the atmosphere depend on the balance between the generation and dissipation of kinetic energy. The kinetic energy of the atmosphere is created through the conversion of the available potential energy and eventually dissipated through frictional processes. The local balance of kinetic energy is governed by three significant terms namely the horizontal flux, the generation and the dissipation of kinetic energy. The mean horizontal flux of kinetic energy is bifurcated into its two constituents, namely the component due to the mean part of the flow and the component due to the eddy part of the flow.

The vertically integrated geographical distributions of significant kinetic energy budget terms are presented in Figure 3. The horizontal flux of kinetic energy (Fig. 3a) depicts a zone of flux divergence extending over the entire south Asian region from the western Pacific to the eastern Arabian Sea. This zone delineates two maxima, the first situated over the Bay of Bengal and the other over the eastern Arabian Sea, respectively. The kinetic energy flux convergence is noticed over the western Arabian Sea, adjoining Arabia and North African regions. These zones of kinetic energy flux transport maxima/minima are situated at the respective locations of entrance/exit regions of the tropical easterly jet.

The adiabatic generation of kinetic energy is presented in Figure 3b. Kinetic energy is basically produced by an ageostrophic component of the flow. Positive magnitudes denote the generation of kinetic energy through the conversion of available potential energy, and negative magnitudes denote the destruction of kinetic energy, i.e., transformation of kinetic energy in to APE. The production regions of kinetic energy (KE) are characterized by strong horizontal flux divergence. The KE generation denotes maxima/minima corresponding to the entrance/exit regions of the tropical easterly jet. The maxima observed off east Africa is due to the presence of a strong ageostrophic flow in that region.

In order to comprehend the characteristic features of kinetic energy generation over the Asian summer monsoon region, the zonal and meridional components of



## KINETIC ENERGY BUDGET JJA 1986-90

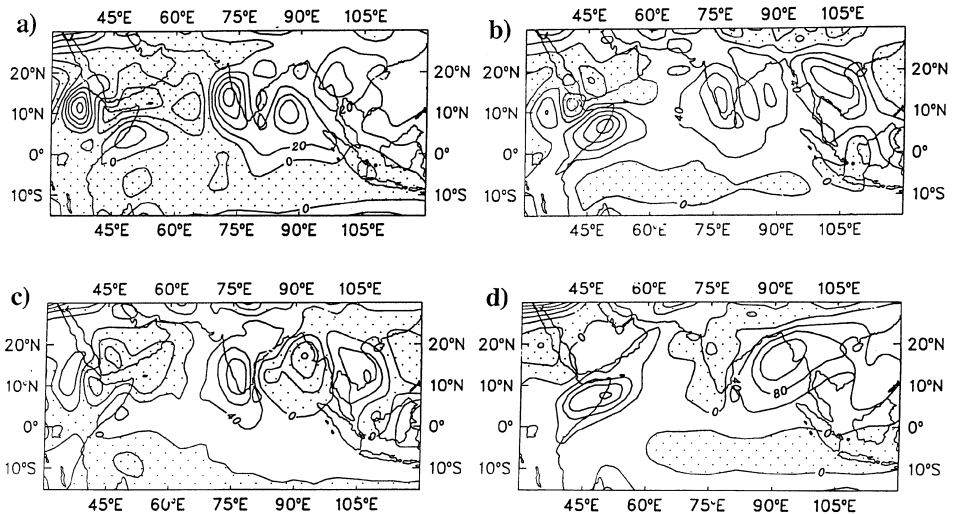


Figure 3

Geographical distribution of vertically integrated kinetic energy budget terms for JJA, 1986–1990 [units:  $10^{-1}$  Watts  $m^{-2}$ ]. (a) Horizontal flux, (b) adiabatic generation, (c) zonal adiabatic generation, (d) meridional adiabatic generation [contour interval for (a): 20; for (b) (c) and (d): 40; negative values are shaded].

adiabatic generation of kinetic energy are also analyzed. Earlier studies (KUNG, 1971) indicated that the zonal component contributes to the destruction/production of kinetic energy in the tropics/extra-tropics and vice versa in the case of the meridional component. Further, these two components oppose each other. The significant features depicted by the zonal component include the production over the eastern Arabian Sea and the adjacent peninsular region, which is a specific feature, confined to the monsoon region only. This is due to the super-geostrophic nature of the zonal flow over the Arabian Sea. It also contributes to the destruction of kinetic energy over the Bay of Bengal due to the sub-geostrophic zonal flow. The meridional component contributes to the destruction of kinetic energy over the Arabian Sea and production over the Bay of Bengal. This is due to the super-geostrophic nature of the meridional flow over the Bay of Bengal and vice versa over the Arabian Sea. According to KUNG (1971), the generation/destruction zones of kinetic energy are characterized by super-geostrophic/sub-geostrophic flow either due to the zonal or meridional component of the wind. As observed earlier in the case of the kinetic energy horizontal flux and adiabatic generation, the summer monsoon circulation is characterized by two centres of action; one over the Bay of Bengal and the other over the eastern Arabian Sea and adjoining south Indian peninsula. The existence of production maxima over these two locations is vital for the maintenance of the flux divergence maxima. Hence, in the

maintenance of the summer monsoon circulation, the adiabatic production of kinetic energy through the action of pressure forces plays a very important role.

The vertical distribution of kinetic energy is analyzed through the sectorial (30°E–120°E) averaged pressure-latitude cross sections of significant kinetic energy budget terms. The horizontal flux of kinetic energy evinces that the monsoon region is characterized by convergence in the lower troposphere and strong divergence in the upper troposphere. However, in the equator region (0–10°N) flux divergence is noted. In the horizontal flux of kinetic energy, the mean component depicts convergence and the eddy component depicts divergence in the upper troposphere of the extra-tropics. However, the role of the Reynolds' stresses on the flux transport of kinetic energy is to counter balance the mean flow transport over the extra-tropics. In the upper troposphere of the summer monsoon regime, the transient eddies are found to supplement the mean flow transport leading to the net flux transport of kinetic energy from the region.

In the free atmosphere, the adiabatic generation of kinetic energy (Fig. 4b) indicates more production over the strong flux divergence regions and destruction/weak production over the flux convergence regions. The kinetic energy production displays two maxima. The primary in the boundary layer and the secondary in the upper troposphere (250–100 hPa). Earlier studies (KUNG, 1971) carried out over

#### KINETIC ENERGY BUDGET JJA 1986-90

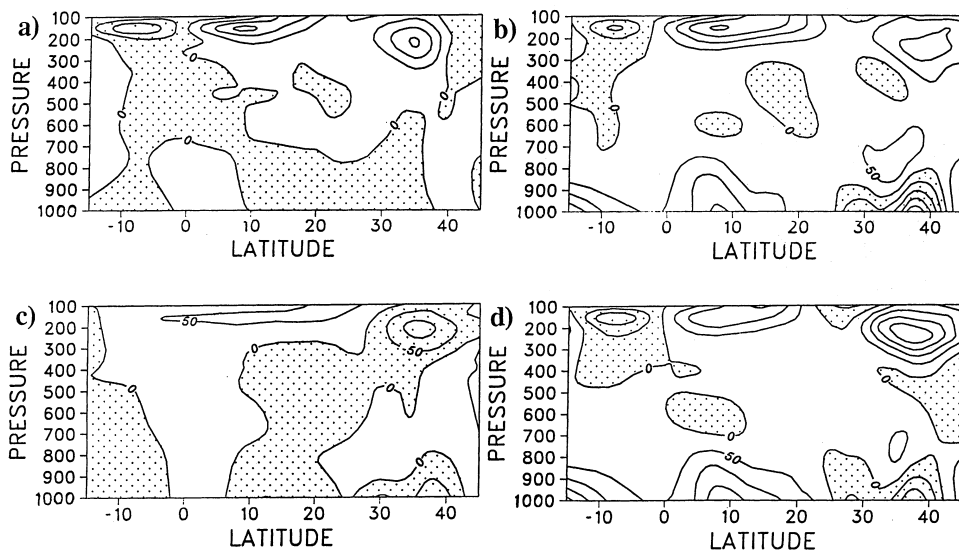


Figure 4

Sectorial (30°E–120°E) mean pressure-latitude cross sections of kinetic energy budget terms for JJA, 1986–1990 [units:  $10^{-4}$  Watt  $\text{kg}^{-1}$ ]. (a) Horizontal flux, (b) adiabatic generation, (c) zonal adiabatic generation, (d) meridional adiabatic generation [contour interval: 50, negative values are shaded].

North America and the tropics (MOHANTY *et al.*, 1989) adduce this aspect, despite the fact that the latter study related to the winter season. The strong generation of kinetic energy in the boundary layer is confined to the tropics only. A plausible explanation is offered by the presence of a strong cross-isobaric flow in the tropics, however, in the extratropics of the Northern Hemisphere kinetic energy destruction/weak production is recognized.

As noticed earlier, the zonal (Fig. 4c) and meridional (Fig. 4d) components oppose each other. The zonal component contributes to the destruction/weak production of kinetic energy in the boundary layer of the monsoon region, and in the upper troposphere (jet level) of the extratropics. Further, it contributes to strong generation/production in the upper levels of the tropics. The salient feature over the monsoon region is that both components contribute to the production of kinetic energy in the upper troposphere. The features depicted by meridional generation in the equator region are strong production in the lower troposphere and destruction/weak production in the upper troposphere over the Southern Hemispheric tropics.

The kinetic energy budget is further analyzed through the area (15°S–45°N, 30°E–120°E) averaged vertical profile presented in Figure 5. It shows that the kinetic energy generation is completely balanced by the dissipation, as the contribution from the horizontal flux terms is insignificant. The monsoon region is characterized by flux convergence in the lower levels and strong flux divergence in the upper levels. The kinetic energy production maxima in the boundary layer and the upper troposphere are similar to those in the investigations (KUNG, 1971; SAVIJARVI, 1980) carried out over North America. The comparison of the boundary layer dissipations over North America, the Atlantic and Europe (SAVIJARVI, 1981) with the Asian summer

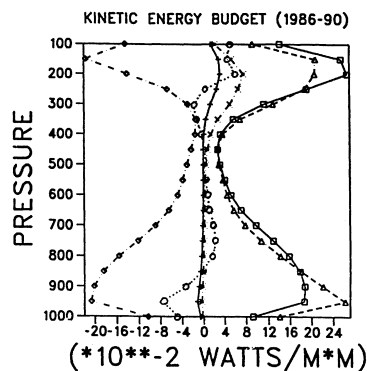


Figure 5

Vertical profile of kinetic energy budget terms for JJA, 1986–1990. [Continuous line with squares indicates adiabatic generation of kinetic energy. Broken lines with + and × indicate eddy and mean horizontal fluxes of kinetic energy, respectively. Broken lines with circles and triangles connote the zonal and meridional adiabatic generation of kinetic energy, respectively. Broken line with diamonds evinces the residue of kinetic energy].

monsoon domain shows higher magnitudes over the monsoon region. This is due to a strong westerly flow over the monsoon domain. The meridional component depicts strong production in the lower as well as the upper troposphere. Further, the magnitudes of meridional generation are one order more than those of zonal generation. The study delineates the monsoon domain as a source region of kinetic energy, which is facilitated through conversion of available potential energy. The

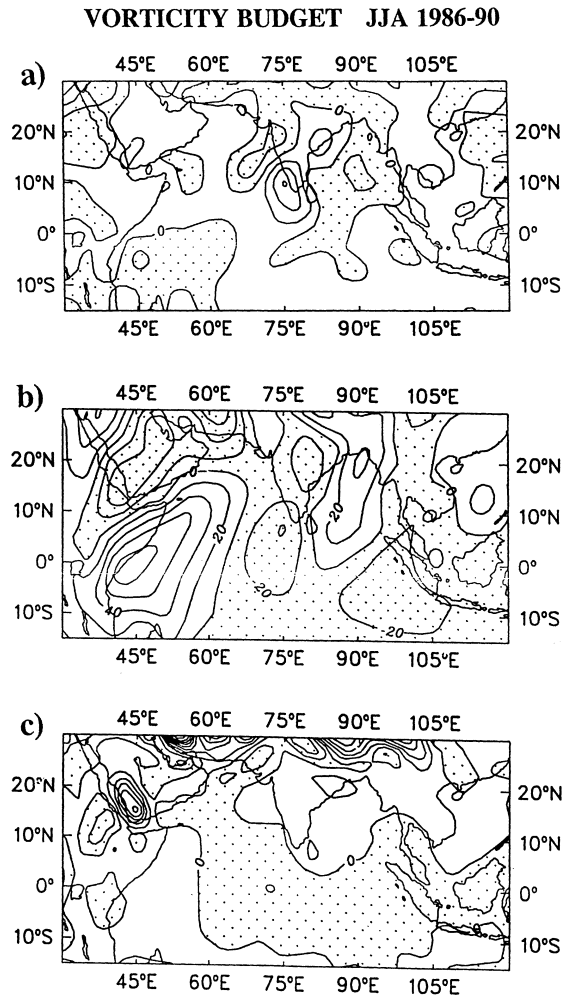


Figure 6

As in Figure 3, but for vorticity budget [units:  $10^{-8} \text{ Nm}^{-3}$ ]. (a) Relative vorticity advection, (b) planetary vorticity advection, (c) generation of vorticity due to stretching [contour interval for (a): 50; for (b) and (c): 20; negative values are shaded].

persistent generation of available potential energy supports a thermally-driven meridional overturning over the monsoon region.

#### 4.3. Vorticity Budget

The characteristic features of the monsoon are further analyzed through the vorticity budget. Earlier studies (HOLOPAINEN and OORT, 1981; CHU *et al.*, 1981) revealed that the horizontal transport and the production terms (stretching and tipping) are significant in the vorticity budget.

The geographical distributions of vertically integrated vorticity budget terms are shown in Figure 6. The relative vorticity advection shows convergence over the Bay of Bengal and north Arabian Sea. It depicts divergence in the southeast Arabian Sea and the adjacent peninsula. The planetary advection indicates divergence over the places of relative vorticity convergence, viz. the Bay of Bengal and off east Africa, as they oppose each other. The east African maximum is due to the strong cross-equatorial meridional monsoonal flow. The monsoon region is characterized by net vorticity advection. The vertically integrated vorticity generation due to stretching is

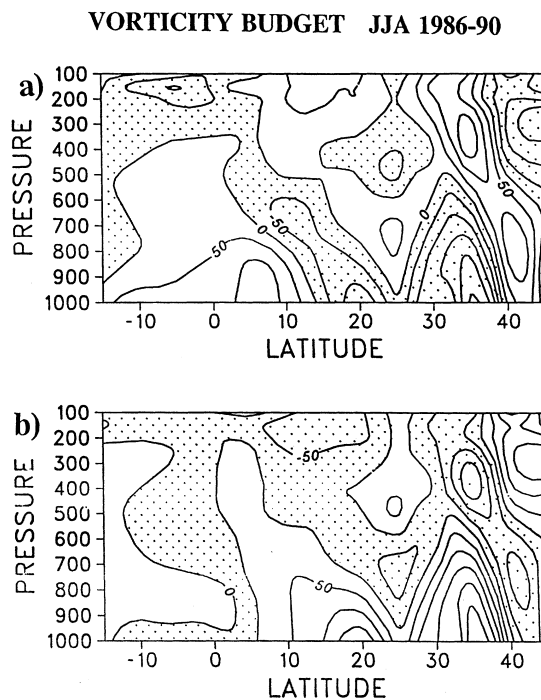


Figure 7

As in Figure 4, but for vorticity budget. [units:  $10^{-12} \text{ s}^{-2}$ ]. (a) Horizontal flux of absolute vorticity, (b) generation of vorticity due to stretching [contour interval: 50, negative values are shaded].

illustrated in Figure 6c. The monsoon region is characterized by strong generation of vorticity. This generation is crucial to maintain the monsoon circulation.

Certain interesting aspects of the vorticity budget are discussed through the cross sections. The sectorial mean cross section of horizontal flux of absolute vorticity (Fig. 7a) demonstrates that the monsoon region is characterized by strong divergence reaching 15°N and strong convergence to the north of that in the lower troposphere. However, in the upper troposphere it connotes strong flux divergence in the monsoon regime, and convergence in the extra-tropics. The lower tropospheric advection is supported by strong generation of vorticity by the stretching term (Fig. 7b). The entire monsoon region is characterized by strong generation of vorticity in the lower troposphere and weak generation/destruction in the upper troposphere. The strong generation in the lower levels may be attributed to cyclonic circulation in association with strong low-level convergence. The stretching term contributes to the generation of anti-cyclonic vorticity to the south of the Tibetan anti-cyclonic circulation, in association with the strong divergence over the prevailing easterly wind regime.

However, over the extra-tropics of the Northern Hemisphere a reverse phenomenon, i.e., production of lower-level anti-cyclonic vorticity and upper-level cyclonic vorticity, is observed. To the north of the Tibetan anti-cyclone in the upper troposphere, convergence of flow is observed in association with the subsidence prevailing over the westerly wind regime. This results in the formation of a strong zone of flux divergence and anti-cyclonic vorticity production in the lower tropospheric levels overlying the sub-tropical high pressure cells. The relative vorticity advection is predominant over the summer monsoon region, which contributes to the horizontal transport of vorticity out of the domain. The planetary vorticity advection also contributes to the horizontal transport from the monsoon domain. The replenishing of vorticity is not effectively balanced by the vorticity generation due to stretching and tilting terms. The budget terms show that the horizontal transportation of vorticity is effectively balanced in the monsoon region by the production of vorticity through sub-grid scale processes such as cumulus convection. Earlier studies (WILLIAMS and GREY, 1973; REED and JOHNSON, 1974; CHU *et al.*, 1981) have delineated that the cumulus convection in the tropics could generate a large apparent source of positive vorticity.

The vertical profile of vorticity budget terms is depicted in Figure 8. The horizontal advection of relative vorticity indicates that the monsoon region is dominated by flux divergence in the lower and upper troposphere. However, the planetary vorticity advection displays, low-level divergence and upper level convergence. The planetary vorticity advection shows a maximum approximating the 950 hPa level and a minimum approximating the 200 hPa level. The vorticity generation due to the stretching of isobars delineates strong production in the lower troposphere and strong dissipation in the upper troposphere. The residue illustrates

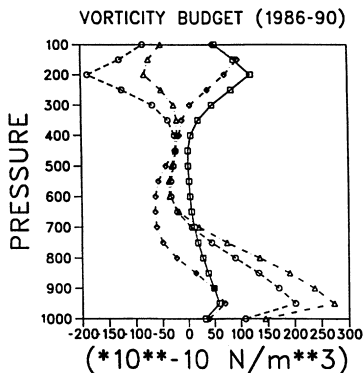


Figure 8

As in Figure 5, but for vorticity budget. [Continuous line with squares indicates horizontal advection of relative vorticity. Broken lines with circles, triangles and diamonds connote horizontal advection of planetary vorticity, vorticity generation due to stretching and residue of vorticity, respectively].

the generation of vorticity in the lower as well as the upper troposphere. However, in the mid troposphere, it contributes to the dissipation.

#### 4.4. Angular Momentum Budget

In the regional angular momentum budget, the horizontal transport terms ( $\Omega$  momentum and relative momentum fluxes), the pressure torque (zonal pressure gradient), and frictional dissipation of momentum govern the balance. The vertically integrated geographical distributions of significant angular momentum budget terms are presented in Figure 9.

The horizontal flux of  $\Omega$  momentum (Fig. 9a) shows strong divergence over the east Arabian Sea and the adjoining peninsular India. Also, flux convergence is depicted over the Tibetan plateau, the Gangetic plains, northeast India, Burma, Bay of Bengal and the west Arabian Sea. The divergence maximum is situated over the peninsular India and the convergence maximum over the head Bay of Bengal. The relative momentum (Fig. 9b) flux distribution shows flux convergence over the entire east Arabian Sea and the adjoining peninsular India with a maximum over the east Arabian Sea. Interestingly, the omega momentum flux opposes relative momentum flux. The monsoon region is characterized by momentum transport into the region in order to balance the surface westerlies against friction. This is illustrated by flux divergence pattern. The vertically integrated geographical distribution of pressure torque (Fig. 9c) indicates that the entire peninsular region is dominant of momentum generation, which is balanced by the flux convergence over the domain. The pressure torque generates momentum along east Africa and adjoining Arabia, and contributes to weak generation/dissipation over the Bay of Bengal, Burma and the western Pacific. The pressure torque delineates maximum generation of momentum over the

## ANGULAR MOMENTUM BUDGET JJA 1986-90

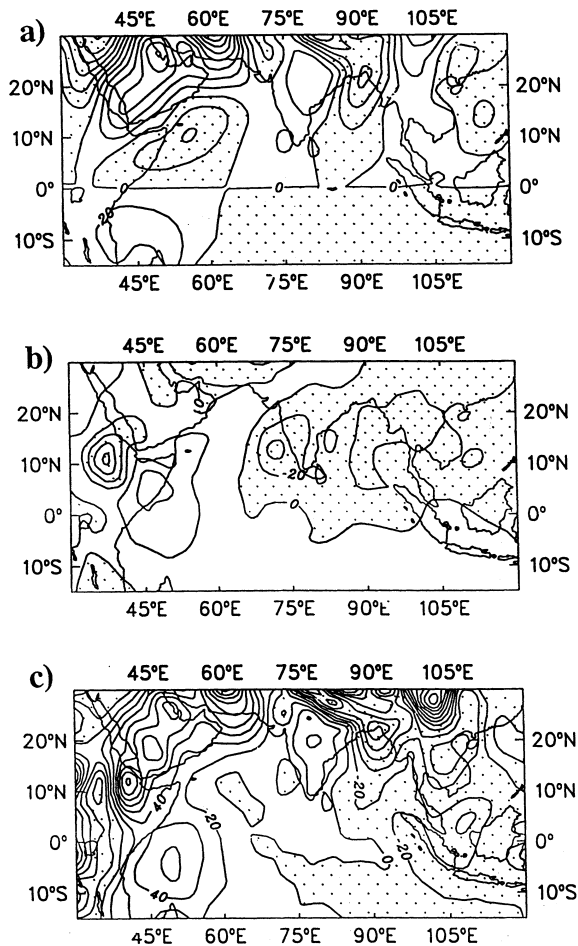


Figure 9

As in Figure 3, but for angular momentum budget. [units:  $10^5 \text{ kg s}^{-2}$ ]. (a) Horizontal flux of omega momentum, (b) horizontal flux of relative momentum, (c) pressure torque [contour interval: 20; negative values are shaded].

south Indian peninsular region. The angular momentum budget is further analyzed through the sectorial mean pressure-latitude cross sections. The  $\Omega$ -momentum cross section (Fig. 10a) exhibits strong flux convergence in the lower levels and strong flux divergence in the upper levels of the Northern Hemispheric (NH) tropics. However, in the Southern Hemispheric tropics and the NH extra-tropics the opposite pattern is seen. As explained earlier, during the monsoon season strong momentum flux convergence is necessary to maintain the surface westerlies. The relative momentum flux delineates the opposite pattern with strong flux convergence in the upper



**ANGULAR MOMENTUM BUDGET JJA 1986-90**

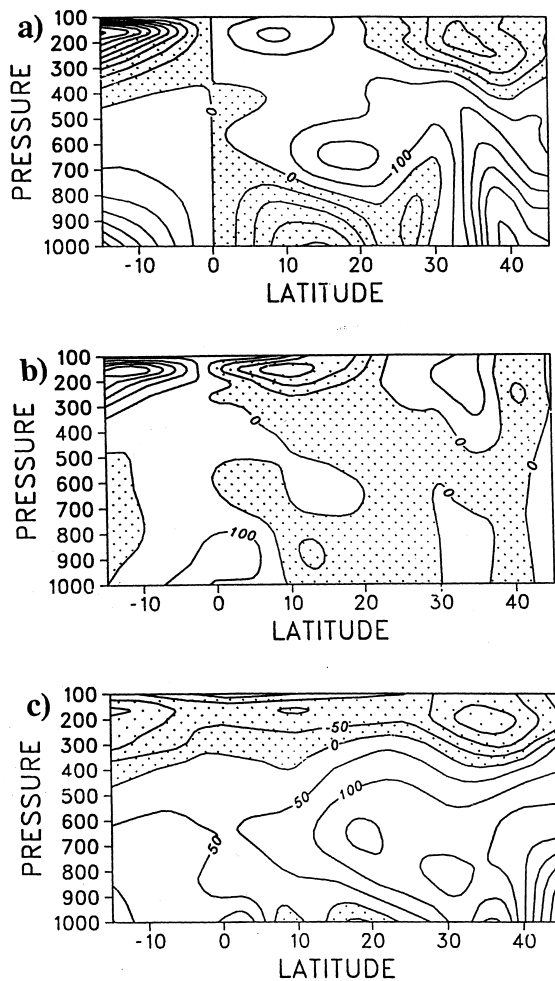


Figure 10

As in Figure 4, but for angular momentum budget. [units:  $10^{14} \text{ m}^4 \text{ s}^{-2}$ ]. (a) Horizontal flux of omega momentum, (b) horizontal flux of relative momentum, (c) pressure torque [contour interval for (a) and (b): 100; for (c): 50, negative values are shaded].

troposphere of the NH tropics. However, in the lower troposphere of the monsoon region a prominent zone of flux convergence is observed between 10°N and 30°N. The pressure torque contributes to the destruction of momentum in the upper troposphere, and generation in the middle troposphere of the monsoon domain. It also contributes to the slight destruction between 5°N and 25°N, and strong generation north of 25°N.

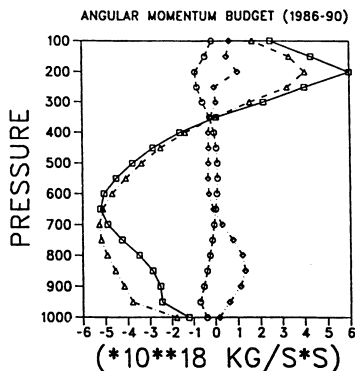


Figure 11

As in Figure 5, but for angular momentum budget. [Continuous line with squares indicates horizontal flux of omega momentum. Broken lines with circles, triangles and diamonds evince horizontal flux of relative momentum, pressure torque and residue of angular momentum].

The area averaged vertical profile of angular momentum budget terms is illustrated in Figure 11. The  $\Omega$  momentum shows strong flux convergence in the lower levels and divergence in the upper levels. The relative momentum flux on the other hand delineates weak convergence in the lower levels and strong convergence in the upper levels. The pressure torque contributes to the destruction of momentum in the upper troposphere and generation in the lower troposphere. The residue of angular momentum contributes to the weak generation of momentum in the lower as well as upper troposphere. Further, it is also seen that the flux convergence due to omega momentum is entirely balanced by the pressure torque over the monsoon domain.

#### 4.5. Heat and Moisture Budgets

The thermodynamical characteristics of the summer monsoon are analyzed through heat and moisture budgets. The vertically integrated horizontal flux of heat is depicted in Figure 12a. The entire monsoon region is dominated by convergence of heat flux. However, strong heat flux divergence is detected off east Africa. The heat flux convergence depicts the maxima over the Bay of Bengal, Indian peninsula and the east Arabian Sea. The adiabatic conversion of available potential energy to kinetic energy (Fig. 12b) denotes that the monsoon region is characterized by the generation of kinetic energy. The zones of excess conversion of kinetic energy are supported by strong convergence of heat flux in the monsoon domain. The adiabatic conversion of kinetic energy from APE delineates maxima over the Bay of Bengal, the peninsular region, the eastern Arabian Sea and the western Pacific, indicating the presence of a strong rising motion over these regions. Further, these are the zones of excess rainfall over the monsoon domain.

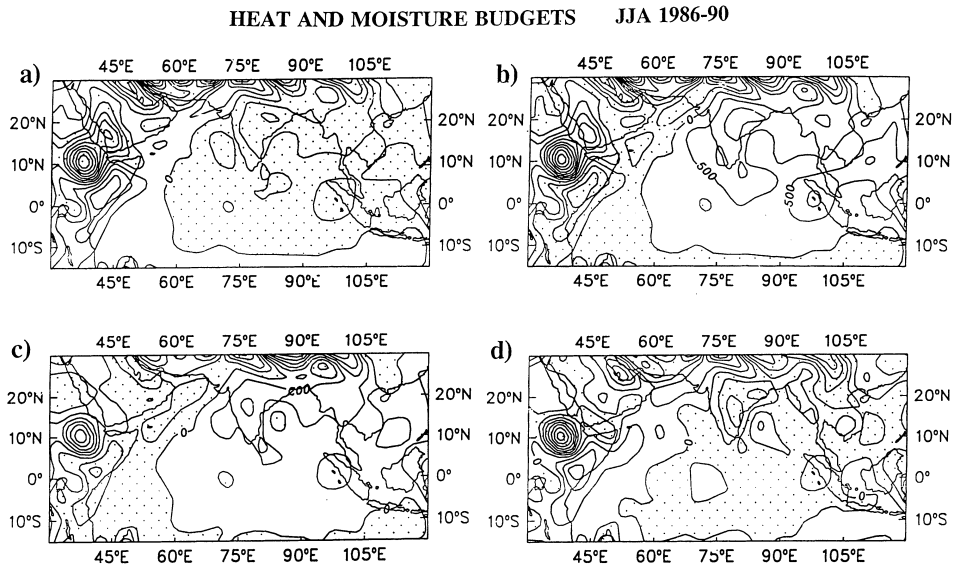


Figure 12

As in Figure 3, but for heat and moisture budgets. [units:  $\text{Watt m}^{-2}$ ]. (a) Horizontal flux of heat, (b) adiabatic conversion of APE to KE, (c) diabatic heating, (d) horizontal flux of moisture [contour interval for (a): 400; for (b): 500; for (c) and (d): 200] [negative values are shaded].

The diabatic heating pattern (Fig. 12c) indicates that the active phase of the monsoon is characterized by the intense diabatic heat sources over the domain. The entire monsoon region is dominated by diabatic heating with maxima over the Bay of Bengal, the east Arabian Sea, the peninsular region, and the western Pacific. These heat sources are identified by strong moisture flux convergence (Fig. 12d) and rainfall as well.

Earlier studies (MOHANTY *et al.*, 1982a,b, 1983; PEARCE and MOHANTY, 1984) reveal that the moisture flux convergence takes place well before the formation of diabatic heat source over the monsoon region. The moisture flux convergence along with diabatic heating plays an important role in modulating the monsoon circulation. The moisture flux transported into the monsoon region is transferred to the middle tropospheric levels through a turbulent exchange mechanism. In the troposphere, the moisture undergoes phase transformation and releases latent heat. Thus the formation of diabatic heat source takes place.

The vertical distribution of heat and moisture budgets are analyzed through their corresponding sectorial means. The sectorial mean of heat flux is depicted in Figure 13a. Strong flux convergence of heat in the lower levels and strong flux divergence of heat in the upper levels are the characteristic features of the monsoon. The lower level flux convergence shows maxima around 20°N and 35°N and the upper level divergence displays maxima around 10°N and 35°N. Heat flux

## HEAT AND MOISTURE BUDGETS JJA 1986-90

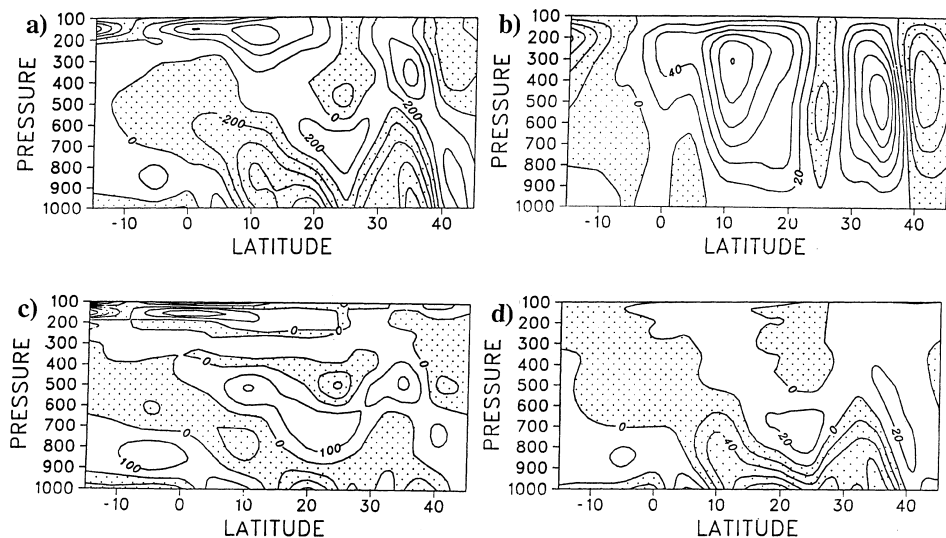


Figure 13

As in Figure 4, but for heat and moisture budgets. [units:  $\text{Watt kg}^{-1}$ ]. (a) Horizontal flux of heat, (b) adiabatic conversion of APE to KE, (c) diabatic heating, (d) horizontal flux of moisture [contour interval for (a): 200; for (b): 20; for (c): 100; and for (d): 20; negative values are shaded].

convergence is seen in the Southern Hemispheric tropics also. The adiabatic conversion of APE to kinetic energy (Fig. 13b) depicts primary maximum around 300 hPa level and another maximum around 500 hPa level over the monsoon region. However in the Southern Hemispheric tropics, negative generation is denoted with maximum around 200 hPa. The adiabatic conversion of APE to KE pattern reveals that the entire monsoon region is dominated by rising motion, which in turn produces APE that ultimately converts to kinetic energy. Hence the monsoon region is characterized as the source region of kinetic energy. Additionally the negative generation in the Southern Hemispheric tropics delineates the subsidence in that region. This confirms the meridional overturning of the monsoon region. Further, the level of maximum in the upper troposphere agrees well with the earlier finding of energy conversion over the tropics (NITTA, 1970). The diabatic heating (Fig. 13c) pattern depicts lower-level maximum. This is however confined between 0–15°N. North of 15°N cooling is observed in the lower levels and strong heating is noticed in the upper levels. The lower-level heating is due to the turbulent transfer of the sensible heat from the warm land and ocean surfaces to the boundary layer. However, the middle tropospheric maximum is due to the release of latent heat through a condensation mechanism. The sectorial mean of horizontal flux of moisture (Fig. 13d) shows a zone of strong convergence in the monsoon region with a maximum between 15°N and 21°N. However, between 0–10°N flux divergence of

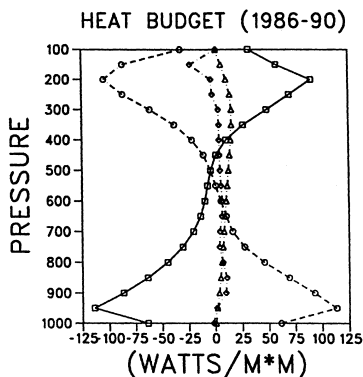


Figure 14

As in Figure 5, but for heat budget. [Continuous line with squares indicates horizontal flux of heat, Broken line with circles, triangles and diamonds connote vertical flux of heat, adiabatic conversion of APE to KE, and diabatic heating, respectively].

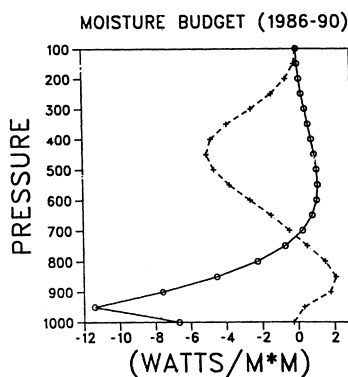


Figure 15

As in Figure 5, but for moisture budget. [Continuous line with circles indicates horizontal flux of moisture and broken line with plus connotes moisture source/sink].

moisture is detected. The vertical structure of various terms in heat and moisture budgets are illustrated in Figures 14 and 15. The horizontal flux of heat (Fig. 14) manifests strong convergence in the lower levels and divergence in the lower levels. On the contrary, the vertical flux of heat indicates the opposite. In effect, the horizontal flux of heat is completely balanced by the vertical flux of heat. An earlier study (MOHANTY *et al.*, 1983) reveals that the horizontal flux of heat is completely balanced by the vertical flux of heat, with maximum convergence in the lower tropospheric levels in the case of horizontal heat flux, and maximum convergence in the upper tropospheric levels in the case of vertical heat flux. The adiabatic conversion of kinetic energy from APE discerns primary maxima around 300 hPa

level and another maximum around 500 hPa level in the monsoon region. Due to the intense rising motion throughout the summer season (JJA), the conversion depicts larger magnitudes in the entire troposphere. The diabatic heating profile shows heating up to 300 hPa and cooling in the upper troposphere. The adiabatic conversion pattern reveals that the entire monsoon region is characterized as the source region of kinetic energy. The diabatic heating profile shows upper tropospheric cooling, apart from lower and middle tropospheric heating, which is attributed to radiational cooling. The moisture flux convergence plays a vital role in the maintenance of monsoon circulation. The organized and strong moisture convergence enhances cumulus convection due to intense vertical motions. The cumulus convection further strengthens the diabatic heating. The intense heat source attracts more moisture flux into the monsoon region as a feedback process. The combined effect leads to the CISK mechanism, which is the characteristic feature of most of the tropical monsoon systems. The significant terms in the moisture budget, namely the horizontal flux of moisture and moisture source/sink, are illustrated in Figure 15. Strong convergence of moisture flux in the lower levels and weak divergence in the upper levels is the characteristic feature of the monsoon region. The moisture source/sink characterizes the monsoon domain as the sink region of moisture.

### 5. Conclusions

The following conclusions are drawn from the above results.

The circulation off east Africa and the adjoining western Indian Ocean determines the strength of cross-equatorial flow and the ageostrophic motions in maintaining the lower tropospheric features of the monsoon. Also, it controls the quantum of heat and moisture flux transport into the monsoon regime.

The circulation over the Bay of Bengal and the eastern Arabian Sea largely determines the upper tropospheric features of the summer monsoon regime. The entrance/exit regions of the tropical easterly jet are characterized by production/destruction of KE, which is essential to maintain outflow/inflow prevailing at the respective locations of the TEJ. It is interesting to note that the eastern Arabian Sea maximum of KE production is maintained by the zonal component, while that over the Bay of Bengal is maintained by the meridional component of the ageostrophic flow. The generation of kinetic energy over the Arabian Sea by the zonal component is a unique feature confined to the monsoon domain only.

The mean circulation of the summer monsoon is characterized by a net vorticity advection from the region of its influence. This observation indicates that the monsoon area is quite unstable during the summer season, with the production of vorticity within the domain itself in order to maintain the circulation. This production is manifested through sub-grid scale processes such as cumulus

convection, unlike other regions where the balance is between the transportation and stretching terms.

In this study, a net momentum flux convergence is observed over the region of low-level monsoon westerlies. Such a distribution is essential to maintain the low level monsoon westerlies against the surface friction. It is also ascertained that pressure torque contributes to the production of momentum and balances the flux convergence over the summer monsoon region.

Further, the summer monsoon domain is characterized by a net convergence of heat and moisture. Also considerable heat energy is generated through the action of adiabatic processes. The combined effect of these processes leads to the formation of strong diabatic heat sources in the region to maintain the monsoon circulation. Ultimately, the study enabled identification of other active zones, which have considerable bearing on the rainfall over the Indian region.

#### *Acknowledgements*

The author is grateful to the ECMWF for providing data, and the National Centre for Medium Range Weather Forecasting, New Delhi for providing computing facilities to carry out the present study. The author also expresses his gratitude to anonymous reviewers, whose comments significantly resulted in improved clarity of the manuscript.

#### REFERENCES

- CHEN, T. C., TZENG, R. Y., and Van LOON, H. (1988), *A Study on the Maintenance of the Winter Subtropical Jet Streams in the Northern Hemisphere*, *Tellus* 40a, 392–397.
- CHU, J. H., YANAI, M., and SUI, C. H. (1981), *Effects of Cumulus Convection on the Vorticity Field in the Tropics. Part-I. The Large-scale Budget*, *J. Meteor. Soc. Japan* 59(4), 535–546.
- GEORGE, L., and MISHRA, S. K. (1993), *An Observational Study on the Energetics of the Onset of Monsoon Vortex, 1979*, *Q. J. R. Meteorol. Soc.* 755–778.
- HOLOPAINEN, E. O., and OORT, A. H. (1981), *Mean Surface Stress Curl over the Oceans as Determined from the Vorticity Budget of the Atmosphere*, *J. Atmos. Sci.* 33, 773–792.
- JARRAUD, M., and SIMMONS, A. J. (1984), *The Spectral Technique*, ECMWF Seminar on Numerical Methods for Weather Prediction, 5–9 September, 1983, Reading, UK, vol. 2, 1–59.
- JULIAN, P. R. (1984), *Some Comparisons of ECMWF IIIB and GFDL IIIB Analyses in the Tropics*, Global Weather experiment News Letter #3, USC-VARP, Washington, DC., 20418, National Academy of Sciences, 20–22.
- KANAMITSU, M. *Some climatological and energy budget calculations using the FGGE level-IIIB analyses during January 1979*. In *Dynamic Meteorology and Data Assimilation Methods* (eds. Bengtsson, L., et al.) (Springer-Verlag 1980), pp. 263–318.
- KRISHNAMURTI, T. N., ARDANUY, P., RAMANATHAN, Y., and PASCH, R. (1981), *On the Onset Vortex of the Summer Monsoon*, *Mon. Weather Rev.* 109, 344–363.
- KUNG, E. C. (1971), *A Diagnosis of Adiabatic Production and Destruction of Kinetic Energy by the Meridional and Zonal Motions of the Atmosphere*, *Q. J. R. Meteorol. Soc.* 97, 61–74.

- KUNG, E. C., and SMITH, P. J. (1974), *Problems of Large-scale Kinetic Energy Balance, a Diagnostic Analysis in GARP*, Bull. Am. Meteor. Soc. 55, 768–777.
- KUNG, E. C., and TANAKA, H. (1983), *Energetics Analysis of the Global Circulation during the Special Observation Periods of FGGE*, J. Atmos. Sci. 40, 2575–2592.
- MOHANTY, U. C., DUBE, S. K., and SINHA, P. C. (1982a), *On the Role of Large-scale Energetics in the Onset and Maintenance of the Summer Monsoon-I: Heat Budget*, Mausam 33, 139–152.
- MOHANTY, U. C., DUBE, S. K., and SINHA, P. C. (1982b), *On the Role of Large-Scale Energetics in the Onset and Maintenance of the Summer Monsoon-II: Moisture Budget*, Mausam 33, 285–294.
- MOHANTY, U. C., DUBE, S. K., and SINGH, M. P. (1983), *A Study of Heat and Moisture Budgets over the Arabian Sea and their Role in the Onset and Maintenance of Summer Monsoon*, J. Meteor. Soc. Japan 61, 208–211.
- MOHANTY, U. C., RAMESH, K. J., and DASH, S. K. (1989), *Energy Transformations in the Tropical Circulation during FGGE Winter*, J. Meteor. Soc. Japan 5(67), 691–704.
- MOHANTY, U. C., and RAMESH, K. J. (1994), *A Study on the Dynamics and Energetics of the Indian Summer Monsoon*. Proceedings of the Indian National Science Academy, 60(A1), 23–55.
- MOHANTY, U. C., RAO, P. L. S., and RAMESH, K. J. (1999), *Evolution and Retreat of the Asian Summer Monsoon over India*, Q. J. R. Meteorol. Soc. (submitted).
- NEWELL, R. E., KIDSON, J. W., VINCENT, D. G., and BOER, G. J. *The General Circulation of the Tropical Atmosphere and Interactions with Extratropical Latitudes*. vol. 1 (The MIT Press 1972).
- NITTA, T. (1970), *A Study of Generation and Conversion of Eddy Available Potential Energy in the Tropics*, J. Meteor. Soc. Japan 48(6), 524–528.
- O'BRIEN, J. J. (1970), *Alternative Solutions to Classical Vertical Velocity Problems*, J. Appl. Met. 9, 197–203.
- PEARCE, R. P. (1979), *On the Concept of Available Potential Energy*, Q. J. R. Meteorol. Soc. 104, 737–755.
- PEARCE, R. P., and MOHANTY, U. C. (1984), *Onsets of the Asian Summer Monsoon 1979–82*, J. Atmos. Sci. 41(9), 1622–1639.
- RAMESH, K. J., MOHANTY, U. C., and RAO, P. L. S. (1996), *A Study on the Distinct Features of the Asian Summer Monsoon during the Years of Extreme Monsoon Activity over India*, Meteorol. Atmos. Phys. 59 (3–4), 173–183.
- RAO, G. V., SCHAUB, W. R., and PUETZ, J. (1981), *Evaporation and Precipitation over the Arabian Sea during Several Monsoon Seasons*, Mon. Weather Rev. 109, 364–370.
- RAO, Y. P. (1976), *South-West Monsoon*, Met. Monograph No. 1/1976, India Meteorological Department, India.
- REED, R. J., and JOHNSON, R. H. (1974), *The Vorticity Budget of the Synoptic-scale Wave Disturbances in the Tropical Western Pacific*, J. Atmos. Sci. 31, 1784–1790.
- SAVIJARVI, H. (1980), *Energy Budget Calculations and Diabatic Effects for Limited Areas Computed from ECMWF Analyses and Forecasts*, Proceedings of the Workshop, Diagnostics of Diabatic Processes, ECMWF, 115–134.
- SAVIJARVI, H. (1981), *The Energy Budgets in North America, North Atlantic and Europe Based on ECMWF Analyses and Forecasts*, ECMWF Tech. Report No. 27.
- SIMMONS, A. J., BURRIDGE, D. M., JARRAUD, M., GIRARD, C., and WERGEN, W. (1989), *The ECMWF Medium Range Prediction Models. Development of the Numerical Formulations and Impact of Increased Resolution*, Meteorol. Atmos. Phys. 40, 28–60.
- WILLIAMS, R. T., and GRAY, W. M. (1973), *Statistical Analysis of Satellite-observed Trade Wind Cloud Clusters in the Western North Pacific*, Tellus 25, 313–336.

(Received December 10, 1999, accepted June 5, 2000)



To access this journal online:

<http://www.birkhauser.ch>

---